

Cellulose nanocrystal/PVA nanocomposite membranes for CO₂/CH₄ separation at high pressure

Zaib Jahan^{a,b}, Muhammad Bilal Khan Niazi^{a,b}, May-Britt Hägg^b, Øyvind Weiby Gregersen^{b,*}

^aSchool of Chemical and Materials Engineering, National University of Sciences and Technology, Islamabad, Pakistan

^bDepartment of Chemical Engineering, Norwegian University of Science and Technology, Norway

ABSTRACT:

Biogas can be used as an alternative energy source in place of conventional fossil fuels. However, for this to happen, it is necessary to optimize biogas production as well as improve the biogas quality. Crystalline nanocellulose (CNC) has excellent mechanical properties as well as a high moisture uptake ability. These properties make CNC a promising candidate to be used as an additive in polyvinyl alcohol (PVA)-facilitated transport membranes (FTMs). The overall objective of this work is to develop CNC/PVA nanocomposite membranes for enhancing the biogas quality through CO₂ capture. The effects of CNC concentration and the pH of the casting solution are investigated to optimize CO₂/CH₄ separation. Membrane characterisation shows that the addition of CNC affects the degree of swelling, crystallinity and thickness of the resulting membranes, while permeation testing showed that the permeance and selectivity for CO₂ increased with the addition of CNC. Membranes produced with 1% CNC and a casting suspension at pH 10 gave the best results under the given set of conditions. The maximum permeance achieved by the formulated nanocomposite membranes was 0.29 m³(STP)/(m²-h-bar), while the selectivity of CO₂ over CH₄ was 43. It was also observed that increasing the feed gas pressure deteriorated the membrane performance.

Keywords:

Crystalline nanocellulose (CNC); Polyvinyl alcohol (PVA); Nanocomposite membranes;
Facilitated transport membranes (FTM); Biogas upgrading

*Corresponding Author: oyvind.w.gregersen@ntnu.no (Øyvind Weiby Gregersen)

Tel.: +47-73594029

Postal address: Department of Chemical Engineering, Norwegian University of Science and
Technology, 7491 Trondheim, Norway

Highlights:

- 1) Degree of swelling of nanocomposite membranes increased by the addition of CNC.
- 2) Thickness of the selective layer increased by increasing the CNC concentration.
- 3) High CNC concentration increased the crystallinity.
- 4) Nanocomposite membranes with 1% CNC show best permeation results.
- 5) At higher pH, membranes show increased CO₂ permeance and selectivity.

1. Introduction

The world is experiencing a rapid increase in population, resulting in higher demands on the industrial production and energy consumption with every passing day. Fossil fuels play a dominant role in fulfilling the current energy demands worldwide. However, the extensive use of fossil fuels is causing global warming because of the release of carbon dioxide [1]. This has driven the public attention toward the utilization of renewable energy sources. Therefore, the development and utilization of non-petroleum renewable energy sources is urgently required to face the challenges of depleting supplies of fossil fuels and the rising threat of global warming [2]. Biogas produced from organic materials can be used as an alternative energy source [3-5]. Biogas is chiefly composed of methane (50–75%) and carbon dioxide (25–50%). Other minor components include water and trace amounts of hydrogen sulphide, ammonia, carbon monoxide, siloxanes, oxygen, nitrogen, and halogenated hydrocarbons [6]. The high CO₂ content in raw biogas reduces its heating value and therefore limits its usefulness. Applications such as vehicle fuel and grid injection require fuels with high purity and high energy content. Biogas can be upgraded by using various methods depending on the end use [2]. Upgraded biogas usually has a higher CH₄ content (>95%). Burning CH₄ results in less CO₂ emission per unit of energy. Furthermore, the use of biogas as a vehicle fuel can reduce the emission of non-methane VOCs by 50%, emission of NO_x by 25%, and significantly reduce particulate emissions [7]. Thus, the use of biogas as an alternative fuel is considered carbon negative and will contribute to reducing the risk of greenhouse gas (GHG) emission.

It is important to develop an optimized upgrading process that consumes less energy and shows higher efficiency, yielding a high methane content in the upgraded biogas. Several classical methods are used to upgrade biogas to the quality of engine fuel [2]. Cryogenic

condensation is used to remove water from raw biogas [8]. Chemical adsorption on iron oxide is a well-known technique used for removing trace amounts of H₂S from biogas [9]. Absorption, water scrubbing, pressure swing adsorption, and membrane-based techniques are used to upgrade biogas by removing CO₂ [2, 9]. Membrane technology has many advantages such as low cost, high energy efficiency, ease of processing, and excellent reliability. Membrane technology is considered a green technology as it does not require any hazardous chemicals [10-12]. Furthermore, it has been reported that membrane technology is advantageous over other techniques for relatively low volumes of gas and raw biogas with high CO₂ content [10]. For most European biogas plants, the average raw biogas volume flow rate is about 500 m³(STP)/h and the fraction of CO₂ present may be as high as 50% (v/v), depending on the source of the biogas. These conditions are well suited to membrane technology for CO₂ separation [13]. Inorganic carbon membranes with well-defined, stable pores offer advantages over organic polymeric membranes for high-pressure applications because of their good chemical and thermal stability in corrosive environments, high gas permeance, and excellent selectivity [14]. However, carbon membranes for pilot and industrial-scale processes are still unavailable owing to high manufacturing costs. Polymeric membranes have the advantages of low cost and easy fabrication. In fact, the membranes available today for use in high-pressure applications are all polymers, primarily cellulose acetates and polyimides.

The potential for the large-scale application of membrane technology is highly dependent on the separation performance of the membrane material. Low cost, ease of fabrication, capacity to work at high pressures, and the ability to prepare composite membranes with various innovative materials give polymeric membranes a clear advantage over other traditional gas separation materials [15, 16]. Some possible examples of innovative membrane materials are polymers with functionalized nanoparticles embedded, fixed site carrier membranes (FSC), or

facilitated transport membranes (FTMs). FTMs have attracted considerable attention in CO₂ separation because they can show both high selectivity and permeance [12]. CO₂ is selectively permeated through the membrane by means of a reversible reaction with complexing agents (carriers) and/or by facilitated transport via solution and dissociation in water with adjusted pH. Non-reactive gases such as N₂ and CH₄ permeate exclusively by the solution diffusion mechanism. An optimal separation can be thus achieved by maximizing the facilitated transport of the preferred component (in this case CO₂), while the other gases are transported only by solution-diffusion. Facilitated transport can thus be enhanced by increasing the degree of water swelling of the membrane material [9], and CO₂ may be selectively transported as a bicarbonate anion through the swollen FTM [17].

Different synthetic materials have been used as active filler materials in FTMs. The addition of bio-fibres is a relatively new idea that can afford environmentally friendly materials because the fibres themselves are environmentally benign and compatible with water-swollen materials [18, 19]. Cellulose is the most abundantly available, biodegradable, and renewable natural polymer in the environment. Nano-sized microfibrils are considered to be the structural building blocks of cellulose. These microfibrils contain both amorphous and crystalline regions [20, 21]. Cellulose can be characterised as a high-molecular-weight homopolymer of β -1,4-linked anhydro-D-glucose units. Cellulose chains exhibit a directional chemical asymmetry along the molecular axis. A hemiacetal unit is present on the chemically reducing end, while a pendant hydroxyl group is attached on the non-reducing side. Bulk cellulose has a degree of polymerisation of up to 20000 [22]. Rod-like nanocrystals are produced by acid hydrolysis of cellulose [22, 23]. Cellulose nanocrystals (CNCs) have attracted the attention of the materials research community because of their unique properties such as low density, high aspect ratio, high mechanical strength, and high specific surface area [20, 24, 25]. CNCs derived from wood are 3–5 nm wide and 100–200 nm long [22].

Thin films of CNCs exhibit high barrier properties, which make them suitable for many applications, mainly in the pharmaceutical, packaging, and paper industries [20, 23, 25, 26]. When CNC-based films are subjected to a humid environment, they show a high degree of swelling. This feature makes CNCs an interesting material for use as a filler in water-swollen polymeric membranes to facilitate the transport of CO₂ [9, 19].

The present work was conducted to develop novel nanocomposite FTMs composed of PVA and CNC. PVA is a water-soluble synthetic polymer that exhibits good thermal and O₂ barrier properties [27, 28]. PVA films have been proven to be a strong candidate for CO₂ gas separation applications [12, 29]. In this work, PVA is mixed with CNCs to develop a high-performance water-swollen FTM. Its hydrophilic nature and good mechanical properties make it a suitable choice for gas separation applications. Experimental work was carried out to determine the optimal concentration of CNCs in PVA FTMs for biogas refining through CO₂ removal. Separation performance was tested at the pressure range of 5–15 bar. Furthermore, the effect of the pH of the casting solution on membrane performance was investigated as an optimization parameter.

2. Experimental Methods

2.1. Materials

Commercial polysulfone (PSf) flat sheet ultrafiltration membranes (MWCO 50,000) were purchased from Alfa Laval. Polyvinyl alcohol M_r 89000–90000 (89% hydrolyzed) and crystalline nanocellulose were purchased from Sigma Aldrich. The average length and width of the CNCs were 130 nm ± 67 nm and 5.9 nm ± 1.8 nm, respectively. Thus, the aspect ratio was 23 ± 12 [30]. NaOH was purchased from VWR. Deionized water was used as the main solvent.

2.2. Casting of membranes

PVA was added to deionized water to obtain a 3wt% PVA mixture. The PVA mixture was then kept at 90°C for 3 h to obtain a transparent solution. The solution was then left rolling overnight at room temperature. The clear PVA solution was then diluted to 2 wt% by adding CNCs and deionized water. The pH was adjusted by using a 0.1M NaOH solution.

Crystalline nanocellulose was added to the 2 wt% PVA solution in different concentrations (0.5, 1.0, 1.5, and 2% CNC) (wt% of PVA). The suspension was mechanically stirred overnight at room temperature, followed by ultra-sonication by using a probe sonicator at 60 W for 10 min. The resultant clear suspensions were kept standing for 2 h at room temperature before casting the membranes.

A nanocomposite membrane containing CNC and PVA was cast to produce a thin, dense, selective layer over a flat PSF sheet by using a dip-coating technique. These supported membranes were then subjected to a heat treatment step, i.e., 3 h of heating at 45°C, followed by 1 h of heating at 105°C [29].

Table1: Membrane codes and corresponding proportions of CNC in PVA membranes

| Membrane | PVA | CNC wt/Dry Weight of PVA | pH of casting solution |
|-------------|-----|--------------------------|------------------------|
| PVA_6pH | 2 g | - | 6 |
| PVA_9pH | 2 g | - | 9 |
| PVA_10pH | 2 g | - | 10 |
| PCNC0.5_6pH | 2 g | 0.5% | 6 |
| PCNC0.5_9pH | 2 g | 0.5% | 9 |

| | | | |
|-------------|-----|------|----|
| PCNC1_6pH | 2 g | 1% | 6 |
| PCNC1_9pH | 2 g | 1% | 9 |
| PCNC1_10pH | 2 g | 1% | 10 |
| PCNC1.5_6pH | 2 g | 1.5% | 6 |
| PCNC1.5_9pH | 2 g | 1.5% | 9 |
| PCNC2_6pH | 2 g | 2% | 6 |
| PCNC2_9pH | 2 g | 2% | 9 |

2.3. Membrane Morphology

The membrane morphology was examined by taking both cross-sectional and surface images by using scanning electron microscopy (HITACHI SU 3500 SEM). The cross-sectional samples were made by freeze cracking the membranes in liquid nitrogen. Prior to taking SEM images, a thin gold layer was coated onto the samples using an AGUR auto-sputter coater at 35 mA for 45 s. Cross-sectional samples were used to measure the thicknesses of the selective layers.

2.4. Moisture uptake

The swelling behaviour of the membrane materials under humid conditions at room temperature was determined. The samples were placed in a 0% RH chamber until an equilibrium state was achieved. The samples were then subjected to a step change from 0% RH to 93% RH. The moisture uptake was measured periodically until equilibrium was established at 93% RH. The degree of swelling was calculated by gravimetric analysis of the samples. Moisture uptake was calculated by measuring the increase in the weight of the

membranes every 24 h for 10 days. The initial “day 0” measurement was taken directly after the membrane was removed from equilibrium with 0% RH at 25°C [31].

2.5. X-ray Diffraction

The crystalline structures of the composite membranes were investigated using a Bruker D8 Focus X-Ray Diffractometer equipped with a LynxEye™ super-speed detector using Cu radiation at a wavelength of 1.5418 Å. The system was operated at 40 kV and 40 mA. The samples were scanned at 2θ angles between 10° and 50° at a step size of 0.02° and scan speed of 2 s/step. The crystallinity index of the membranes was calculated as reported in the literature [32]. The Origin 8.1 software was used for the integration of peaks. The area under the curve from 10° to 50° in the XRD spectrum was considered as the total area.

2.6. Permeation test

The separation performance of the PVA/CNC nanocomposite membranes was tested in a specially designed high-pressure membrane rig where the feed pressure could be set within the range of 1–80 bar [33]. Membranes of different composition and pH were tested for CO₂ permeance and selectivity. A premixed feed gas (40 mol% CO₂ and 60 mol% CH₄ gas mixture AGA AS) was humidified and then supplied to the membrane module. A flat sheet type membrane module was mounted in a thermostatic cabinet with a temperature control system. Experiments were conducted at different feed pressures: 5, 10, and 15 bar. The relative humidity (RH) was maintained at 93%. Keeping all other parameters constant, i.e., flow rates of feed and sweep gas streams, relative humidity (RH), and temperature, the effect of different pressures on the performance of the FTM membranes was investigated. The composition of the permeate gas was analysed online by a gas chromatograph.

3. Results and discussion

3.1 Membrane characterization

3.1.1. Membrane morphology

The membrane morphology was examined with field emission scanning electron microscopy. Fig. 1 (a) shows a smooth, defect free surface image of the PVA membrane containing 1% CNC. Hence, the addition of CNC does not affect the surface morphology of the composite membranes. Fig. 1 (b) shows the cross sectional view of composite membranes with 1% CNC cast onto a PSf support. The samples were taken from different parts of the membrane and readings were taken for each sample. The average observed thickness of the selective layer was 800nm. When the concentration of CNC was increased, the thickness of the selective layer also increased. Fig. 1 (c) shows variation in thickness with increasing concentration of CNC. The increase in thickness is due to the increased viscosity of the casting suspension with higher concentrations of CNC. The higher viscosity yields higher suspension thickness on the support after dip-coating and therefore increased membrane thickness.

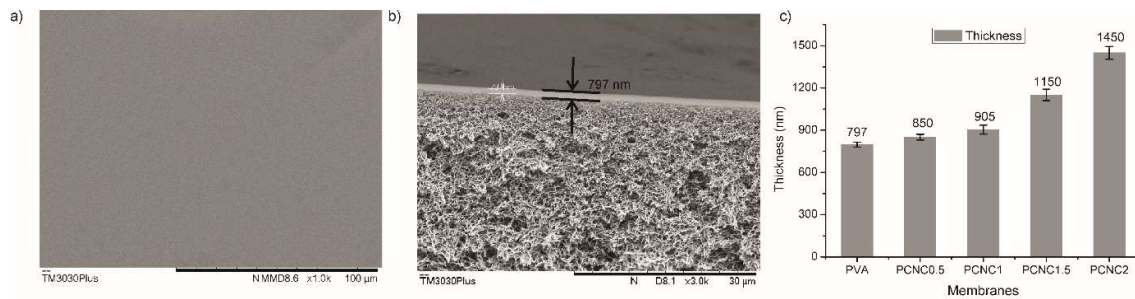


Fig. 1. SEM images of PVA/CNC nanocomposite membranes showing (a) surface morphology, (b) cross-sectional view and thickness of the selective layer, and (c) graphical representation of the effect of increasing concentration of CNC on the thickness of the membrane selective layer.

3.1.2. Moisture uptake

Moisture uptake of all PVA/CNC composite membranes at 93% RH is presented in Fig. 2. The effect of the CNC concentration and the pH of the casting membrane suspension on the moisture absorption of composite membranes under high humidity conditions was investigated. Fig. 2 (a, b) shows the % increase in weight due to moisture uptake over 10 days. The maximum moisture absorption occurred after 4 days for all membranes. PVA_6pH was also analysed as a reference sample to study the effect of pH. All reported composite membranes absorbed water at 93% RH for 4 days except for PVA_6pH, which absorbed water for 5 days. The moisture uptake increased with the pH of the membrane suspension. Pure PVA absorbed almost twice the amount of water after four days at pH 9 compared to that at pH 6, i.e., $70.4 \pm 2\%$ and $35 \pm 1.0\%$, respectively. Similarly, PCNC1_10pH absorbed more moisture than PCNC1_9pH, i.e., $83.4 \pm 1.2\%$ and $80.2 \pm 1.2\%$, respectively. At pH 9, the addition of 1% CNC gave the maximum swelling, i.e., $80.2 \pm 1.2\%$. In contrast, all other composite membranes containing CNC absorbed lower amounts of moisture than PVA_9pH. This reduction in moisture uptake with the addition of CNC is attributed to the reinforcing effect of the CNC. It acts as a reinforcement in a polymer, mechanically restraining the swelling, thereby decreasing the moisture uptake after the addition of CNC to PVA membranes. Moreover, the reduction in moisture uptake with the addition of CNC at higher pH can be attributed to intermolecular hydrogen bonding of highly active nanocellulose with PVA. This renders the membrane tighter and with a reduced amount of moisture absorption sites [34]. The reduced swelling of PVA/CNC nanocomposite membranes may also be enhanced by an increase in the degree of crystallinity of the membranes with the addition of CNC (Fig. 3). It is important to have maximum swelling at relatively high humidities, i.e., 93% RH, for CO₂ membrane applications. Therefore, higher permeation is expected at lower CNC concentrations in PVA membranes at high pH.

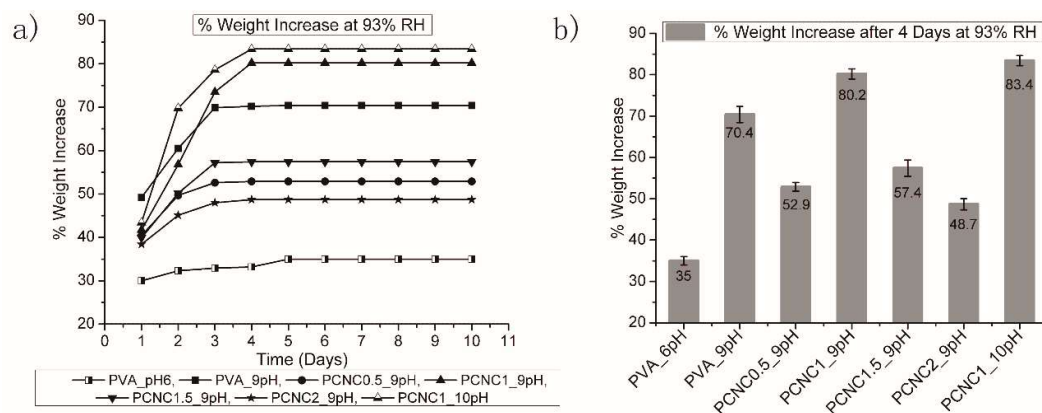


Fig. 2. Moisture uptake of PVA/CNC composite membranes a) at 93% RH, and b) maximum % weight increase after 4 days at 93% RH

3.1.3. X-ray Diffraction

The XRD patterns of all composite membranes at 93% RH are shown in Fig. 3 (a, b). The crystallinity of pure PVA at pH 6 and pH 9, and PVA/CNC composite membranes were calculated. The characteristic peak of PVA at 19.5° was observed for all the composite membranes representing the (110) plane of the semi-crystalline region of partially hydrolyzed PVA [35]. The pure PVA membrane exhibited slightly lower crystallinity at pH 6, i.e., 57.0 ± 0.41 . The addition of CNC to the PVA matrix increased the intensity of the (110) peak, indicating higher crystallinity. Furthermore, the intensity of the CNC peak at a 2θ angle of 23° also increased with CNC concentration in PVA composite membranes. In PCNC2_9pH, the intensity of the CNC peak at a 2θ angle of 23° suppressed the PVA peak at 19° . The results revealed that the crystallinity of the PVA/CNC composite membranes was directly proportional to the CNC content in the formulation. PCNC2_9pH showed the maximum crystallinity at 68.8 ± 0.59 , while PCNC0.5_9pH showed the lowest value at 60.8 ± 0.47 . The peak associated with CNC was observed, even for samples with low CNC content, i.e., 0.5% CNC (wt/wt PVA), suggesting an increase in crystallinity. This increase in crystallinity after the addition of CNC to PVA nanocomposite membranes at 93% RH can be attributed to the

contribution of both PVA and CNC to the overall crystallinity. Moreover, the addition of nanocellulose will also increase the number of nucleating agents, resulting in a higher quantity of small crystallites being bundled together [34].

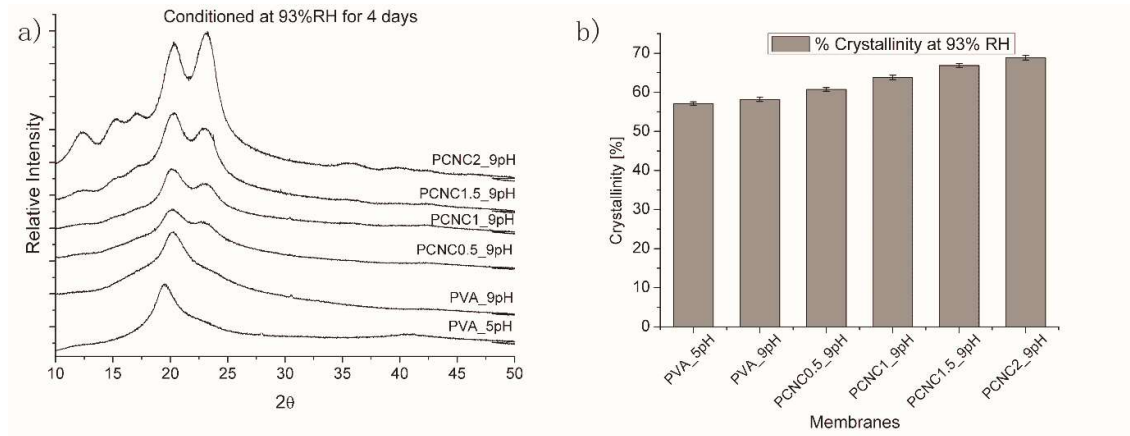


Fig. 3. XRD patterns and crystallinity of PVA/CNC composite membranes a) conditioned at 93% RH for 4 days, and b) percent crystallinity at 93% RH after 4 days.

The increase in crystallinity reduces the number of amorphous domains in the polymer matrix. The structure of the polymer becomes less flexible, reducing the chain mobility. Hence, the overall performance of the FTM is reduced. An increase in moisture uptake helps to rearrange the molecular domains, and hence, causes an increase in crystallinity. However, the presence of water in the water-swollen membranes increases chain flexibility. Therefore, membranes are expected to perform best at the optimum amount of CNC and a high value of RH.

3.2. Permeation Test

3.2.1. Effect of addition of CNC

The homogeneous and defect-free PVA/CNC nanocomposite membranes were cast on PSf supports. Different amounts of CNC (0.05, 1.0, 1.5, and 2 wt%) were added to a 2 wt% PVA solution in order to optimize the membrane composition for CO₂/CH₄ separation. The pH of the PVA/CNC solution was held at 6, while all membranes were cast. Fig. 4.1 describes the effect of the addition of CNC to 2% PVA nanocomposite membranes on CO₂ permeance and selectivity at pH 6. Fig. 4.2 shows the effect of the addition of CNC on membrane performance at pH 9. When compared to the pure PVA membrane, it was found that the addition of CNC has a positive influence on membrane performance. Permeation testing shows that both CO₂ permeation and selectivity increased after the addition of CNC to the PVA membrane. The optimum performance was achieved by the addition of 1 wt% CNC. CNC was added to improve the swelling behaviour and facilitate the transport through the membranes. Water plays an important role in the CO₂ transport mechanism through FTMs. It reacts with CO₂ and converts it first into carbonic acid and subsequently into bicarbonate. In addition, water helps to swell the membrane and increase its free volume by separating polymer chains. This increased free volume results in enhanced non-selective diffusive transport of CO₂ and N₂ [36]. Furthermore, it is assumed that the addition of nanoparticles also provides pathways for nonselective gas diffusion through the polymer matrix. On the basis of molecular sizes, CO₂ and CH₄ have almost equal chances to diffuse through these pathways. In the case of water-swollen FTMs, the selectivity of CO₂ over CH₄ is significantly increased due to the high solubility of CO₂ in water. However, further addition of CNC beyond 1% resulted in a drop in both permeability and selectivity. This may be due to a decrease in the moisture uptake ability, an increase in crystallinity, and/or an increase in the overall thickness of the selective membrane layer. The addition of 2% CNC to a pure PVA membrane increased the overall thickness from 750 nm to 1450 nm (as shown in Fig. 1c). While considering the effect of CNC addition, after the addition of 1% CNC to a PVA

membrane, the thickness of the membrane was 900 nm and the CO₂ permeance increased as well (0.20 m³(STP)/(m²-bar-h)). However, after the addition of 2% CNC, the thickness of the membrane increased to 1450 nm, while the permeance decreased to 0.14 m³(STP)/(m²-bar-h).

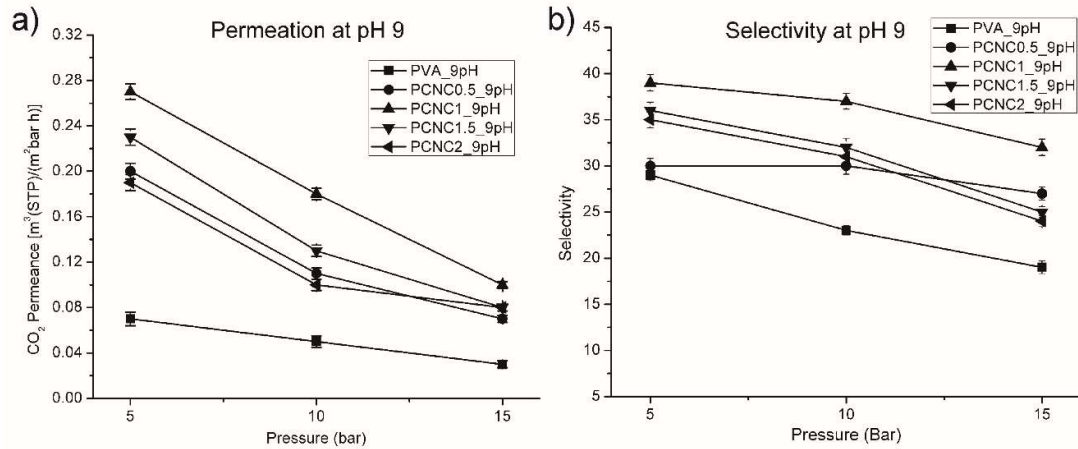


Fig. 4. Different concentrations of crystalline nanocellulose (CNC) in 2 wt% PVA at different pH (a) CO₂ permeability at different pressures at pH 6 and (b) CO₂ selectivity over CH₄ at pH 6. (c) CO₂ permeability at different pressures at pH 9 and (d) CO₂ selectivity over CH₄ at pH 9.

3.2.2. Effect of Feed Pressure

Each membrane has been tested against different pressures: 5, 10, and 15 bar. Fig. 5 shows the effect of varying the feed partial pressure on membrane performance. By increasing the pressure, both selectivity and permeability decreased. The same effect was observed for all membranes tested at pH 6, 9, and 10. For 1% CNC, pH 9, and a feed pressure of 5 bar, the CO₂/CH₄ selectivity increased to 39 and a permeance of 0.27 m³(STP)/(m² h bar) was achieved. However, at feed pressure of 15 bar, the selectivity was 31 and the permeance decreased to 0.11 m³ (STP)/(m²-h-bar). Results from the permeation tests show that both permeation and selectivity decreased after increasing the feed partial pressures. In water-

swollen facilitated transport membranes, this decrease in CO₂ permeation and selectivity could be due to the following reasons: 1) The performance of water-swollen membranes is highly dependent on the relative humidity in the gas stream [37]. It has been previously reported that by increasing the feed pressure, the flux of both CO₂ and water can be increased. Thus, the high feed pressure results in low water content in the membrane even at high %RH [38]. The lower absolute water vapour content in the gas stream at high feed pressure could cause a reduction in both CO₂ permeance and selectivity [37]. 2) Moreover, plasticization of the polymeric membranes at high pressure may lead to further reduction in CO₂ permeance and selectivity. High pressure compresses the swollen membrane and results in the loss of water and a subsequent decrease in polymer chain flexibility and free volume for diffusive transport.

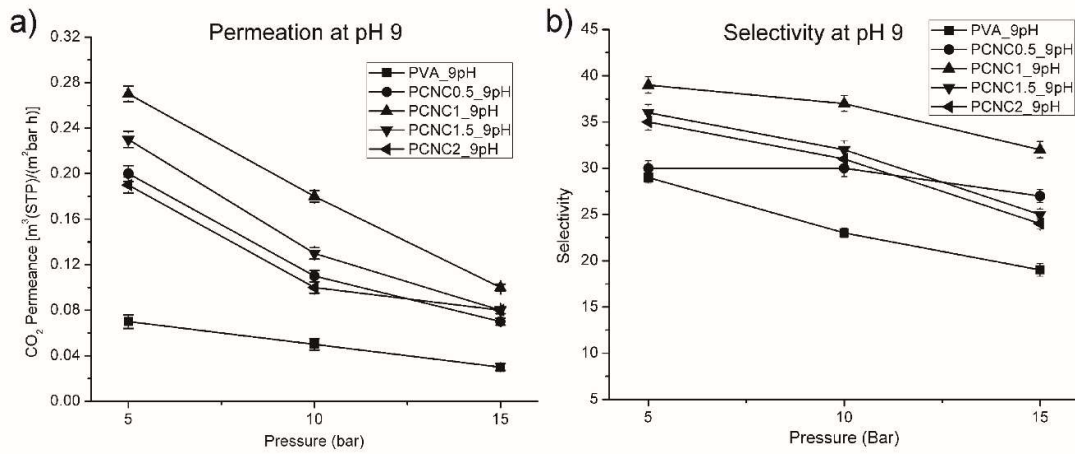


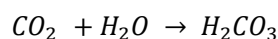
Fig. 5. Change in permeance and selectivity of PVA/CNC nanocomposite membranes with feed pressure (a) CO₂ permeance with increasing pressure and (b) CO₂/CH₄ selectivity with increasing pressure.

3.2.3. Effect of pH

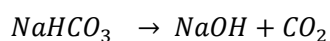
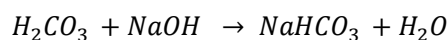
It has been reported in previous studies that increasing pH has a positive influence on both swelling behaviour and facilitated transport through polymeric membranes [29, 39]. In order to achieve high membrane performance, the pH of all casting solutions was adjusted to 9 and 10 by adding 0.1 M NaOH solution. Casting suspensions having pH values higher than 10 became remarkably more viscous owing to the flocculation of the CNC. Viscous solutions resulted in comparatively thicker and non-uniform membranes and were hence not tested for their permeation performance. Fig. 5 describes membrane performance at pH 9. Permeation tests showed that the membrane performance increased with increasing pH. 1% CNC showed the maximum permeation and the highest selectivity for CO₂ over CH₄. Fig. 6 shows the effect of the pH of the casting suspension on membrane performance. Membranes with 1% CNC were tested at pH 6, 9, and 10. The permeance of 1% CNC at pH 10 is four times more than that of the pure PVA membrane without the addition of CNC, tested at the same conditions. However, the selectivity increased from 28 to 43.

In FTMs, CO₂ diffuses by a reversible reaction in the presence of water molecules. At higher pH, increased hydroxyl content results in more CO₂ dissolving in water-swollen membranes and dissociating into bicarbonate ions. These bicarbonate ions then diffuse through the polymer matrix and release CO₂ on the permeate side [33, 39]. This phenomenon can be explained by using chemical equations as given below.

In the first step, CO₂ reacts with water to produce bicarbonate ions.



These bicarbonate ions then react reversibly with NaOH.



The increased pH contributes to CO₂ transport via both the reaction mechanism and through solution diffusion. At high pH, more hydroxyl ions are available, which react with more CO₂ molecules and increase CO₂ transport through the membrane. Furthermore, the higher pH increases the degree of swelling, resulting in the opening of more amorphous regions in the PVA matrix, leading to increased CO₂ transport by solution diffusion.

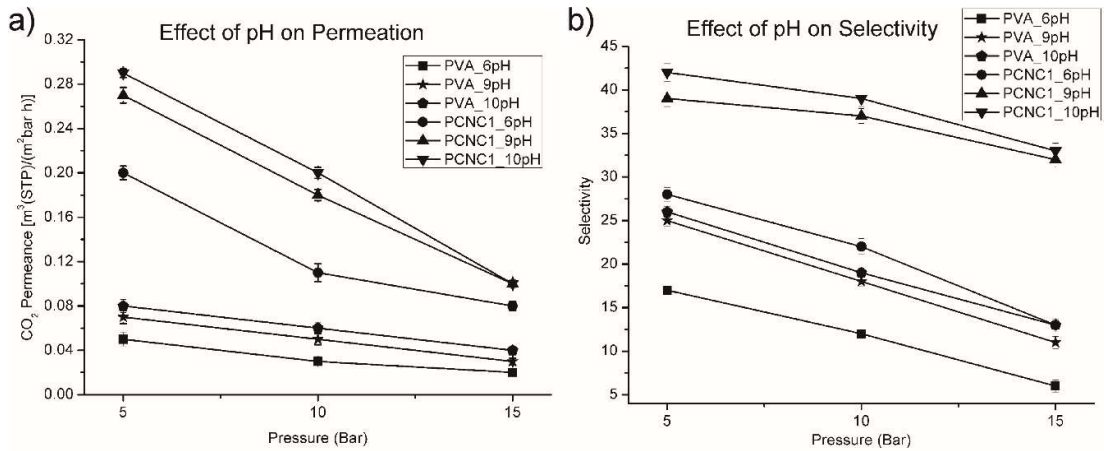


Fig. 6. Membrane performance changes with increases in pH: (a) effect of pH on permeation of CO₂ and (b) effect of pH on CO₂ selectivity.

Different fillers have been reported in the literature for their beneficial effects on gas permeability through polymeric membranes. The addition of nanoparticles such as ZIF-8, NH₂-MOF-199, NH₂-MIL-125, and CNTs in polymeric matrices has shown rapid increases in gas permeability (Table 2). However, higher filler loadings of such nanomaterials are required to increase the permeability and a corresponding loss of selectivity is observed. The CNC used in this work is beneficial, as the addition of very small amounts of CNC showed rapid increases in both permeability and selectivity. The results of the permeability and selectivity testing in this work at 5 bar have been compared to different fillers and polymers that have been used in recent studies in Table 2.

Table 2. Comparison of permeability and CO₂/CH₄ selectivity of different fillers used in polymeric membranes. The experimental conditions are not identical in these literature data.

| Polymer | Fillers | Pressure (bar) | Permeability Barrer | CO ₂ /CH ₄ Selectivity | Reference |
|--------------------|------------------------------|-------------------|------------------------|---|-----------|
| PVA | - | 5 | 12.9* | 25 | This work |
| PVA | CNC | 5 | 70* | 39 | This work |
| PU | - | 4 | 2.7 | 7.5 | [40] |
| PU | ZIF-8 | 4 | 14.2 | 13.7 | [40] |
| 6FDA-duren | - | 3.5 | 468.0 | 7.0 | [41] |
| 6FDA-duren | ZIF-8 | 3.5 | 1462.8 | 9.0 | [41] |
| Matrimid® 9725 | - | 9 | 6 | 30 | [42] |
| Matrimid @ 9725 | NH ₂ -MIL 125 | 9 | 50 | 37 | [42] |
| 6FDA-ODA | - | 10 | 14 | 42 | [43] |
| 6FDA-ODA | NH ₂ -MOF- 199 | 10 | 27 | 52 | [43] |

*Calculated on the basis of dry selective thickness.

4. Conclusions

Polyvinyl alcohol-facilitated transport membranes (FTMs) have been investigated for their CO₂ capture performance as a function of the concentration of crystalline nanocellulose (CNC) and the pH of the casting suspension. When compared to a pure PVA membrane, increases in both permeance and selectivity were observed upon the addition of CNC. Hence, CNC can be used as an additive in facilitated transport membranes. The performance of these membranes can be further improved by increasing the pH of the casting suspension. The

degree of swelling highly influenced the performance of the membrane. However, the swelling properties of PVA/CNC nanocomposite membranes depend on both the concentration of CNC and the pH of the casting solution. Surface morphology remains unaffected, but increasing the concentration of CNC affects the thickness of the selective layer. The addition of CNC also influences crystallinity. A remarkable increase in crystallinity upon the addition of higher concentrations of CNC adversely affects the membrane performance.

Acknowledgments

The authors would like to thank Arne Lindbråthen and Xuezhong He for their kind assistance during permeation experiments. Thanks also to Magnus Rotan in the Department of Material Science and Engineering of Norwegian University of Science and Technology for XRD analysis. One of the authors (Zaib Jahan) was supported by the National University of Sciences and Technology (NUST) Islamabad, Pakistan. This research has also been co-funded by the Norwegian Research Council project: NanoMBE, project number 239172 of the Nano2021 program.

This research did not receive any other specific grants from funding agencies in the public, commercial, or not-for-profit sectors.

References:

[1] M. Miltner, A. Makaruk, M. Harasek, Review on available biogas upgrading technologies and innovations towards advanced solutions, *Journal of Cleaner Production*, (2017).

- [2] D. Andriani, A. Wresta, T. Atmaja, A. Saepudin, A Review on Optimization Production and Upgrading Biogas Through CO₂ Removal Using Various Techniques, in: *Appl. Biochem. Biotechnol.*, 2014, pp. 1909-1928.
- [3] I. Angelidaki, L. Ellegaard, Codigestion of manure and organic wastes in centralized biogas plants - Status and future trends, *Appl Biochem Biotech*, 109 (2003) 95-105.
- [4] Yadvika, Santosh, T.R. Sreekrishnan, S. Kohli, V. Rana, Enhancement of biogas production from solid substrates using different techniques - a review, *Bioresource Technol*, 95 (2004) 1-10.
- [5] A. Schluter, T. Bekel, N.N. Diaz, M. Dondrup, R. Eichenlaub, K.H. Gartemann, I. Krahn, L. Krause, H. Kromeke, O. Kruse, J.H. Mussnug, H. Neuweiger, K. Niehaus, A. Puhler, K.J. Runte, R. Szczepanowski, A. Tauch, A. Tilker, P. Viehover, A. Goesmann, The metagenome of a biogas-producing microbial community of a production-scale biogas plant fermenter analysed by the 454-pyrosequencing technology, *J Biotechnol*, 136 (2008) 77-90.
- [6] E. Ryckebosch, M. Drouillon, H. Veruieren, Techniques for transformation of biogas to biomethane, *Biomass Bioenerg*, 35 (2011) 1633-1645.
- [7] E. Porpatham, A. Ramesh, B. Nagalingam, Investigation on the effect of concentration of methane in biogas when used as a fuel for a spark ignition engine, *Fuel*, 87 (2008) 1651-1659.
- [8] N. Abatzoglou, S. Boivin, A review of biogas purification processes, *Biofuel Bioprod Bior*, 3 (2009) 42-71.
- [9] M. Karaszova, J. Vejrazka, V. Vesely, K. Friess, A. Randova, V. Hejtmanek, L. Brabec, P. Izak, A water-swollen thin film composite membrane for effective upgrading of raw biogas by methane, *Separation and Purification Technology*, 89 (2012) 212-216.
- [10] R.W. Baker, K. Lokhandwala, Natural gas processing with membranes: An overview, *Ind Eng Chem Res*, 47 (2008) 2109-2121.

- [11] S.K. Wahono, R. Maryana, A. Kismurtono, Biogas Purification Process to Increase Gen-Set Efficiency, *Aip Conf Proc*, 1169 (2009) 185-189.
- [12] L.Y. Deng, M.B. Hägg, Techno-economic evaluation of biogas upgrading process using CO₂ facilitated transport membrane, *Int J Greenh Gas Con*, 4 (2010) 638-646.
- [13] A. Makaruk, M. Miltner, M. Harasek, Membrane biogas upgrading processes for the production of natural gas substitute, *Separation and Purification Technology*, 74 (2010) 83-92.
- [14] A.F. Ismail, L.I.B. David, A review on the latest development of carbon membranes for gas separation, *Journal of Membrane Science*, 193 (2001) 1-18.
- [15] T.C. Merkel, B.D. Freeman, R.J. Spontak, Z. He, I. Pinnau, P. Meakin, A.J. Hill, Ultraparable, reverse-selective nanocomposite membranes, *Science*, 296 (2002) 519-522.
- [16] S. Basu, A.L. Khan, A. Cano-Odena, C.Q. Liu, I.F.J. Vankelecom, Membrane-based technologies for biogas separations, *Chem Soc Rev*, 39 (2010) 750-768.
- [17] R. Quinn, J.B. Appleby, G.P. Pez, New Facilitated Transport Membranes for the Separation of Carbon-Dioxide from Hydrogen and Methane, *Journal of Membrane Science*, 104 (1995) 139-146.
- [18] L. Ansaloni, J. Salas-Gay, S. Ligi, M.G. Baschetti, Nanocellulose-based membranes for CO₂ capture, *Journal of Membrane Science*, 522 (2017) 216-225.
- [19] Z. Jahan, M.B.K. Niazi, Ø.W. Gregersen, Mechanical, thermal and swelling properties of cellulose nanocrystals/PVA nanocomposites membranes, *J Ind Eng Chem*, (2017).
- [20] M.J. Cho, B.D. Park, Tensile and thermal properties of nanocellulose-reinforced poly(vinyl alcohol) nanocomposites, *J Ind Eng Chem*, 17 (2011) 36-40.
- [21] Y.C. Ching, T.S. Ng, Effect of Preparation Conditions on Cellulose from Oil Palm Empty Fruit Bunch Fiber, *Bioresources*, 9 (2014) 6373-6385.

- [22] X.D. Cao, L.A. Lucia, Fabrication and properties of cellulose/cellulose nanocrystal composite nanofibers, *Abstr Pap Am Chem S*, 239 (2010).
- [23] A. Dufresne, Nanocellulose: a new ageless bionanomaterial, *Mater Today*, 16 (2013) 220-227.
- [24] S.Y. Lee, D.J. Mohan, I.A. Kang, G.H. Doh, S. Lee, S.O. Han, Nanocellulose reinforced PVA composite films: Effects of acid treatment and filler loading, *Fiber Polym*, 10 (2009) 77-82.
- [25] Y. Habibi, L.A. Lucia, O.J. Rojas, Cellulose Nanocrystals: Chemistry, Self-Assembly, and Applications, *Chem Rev*, 110 (2010) 3479-3500.
- [26] G. Siqueira, J. Bras, A. Dufresne, Cellulosic Bionanocomposites: A Review of Preparation, Properties and Applications, in, MDPI AG, Basel, 2010, pp. 728-765.
- [27] P. Alexy, D. Kachova, M. Krsiak, D. Bakos, B. Simkova, Poly(vinyl alcohol) stabilisation in thermoplastic processing, *Polym Degrad Stabil*, 78 (2002) 413-421.
- [28] Y. Shang, Y.L. Peng, Research of a PVA composite ultrafiltration membrane used in oil-in-water, *Desalination*, 204 (2007) 322-327.
- [29] M. Saeed, L.Y. Deng, CO₂ facilitated transport membrane promoted by mimic enzyme, *Journal of Membrane Science*, 494 (2015) 196-204.
- [30] S.N. Molnes, I.P. Torrijos, S. Strand, K.G. Paso, K. Syverud, Sandstone injectivity and salt stability of cellulose nanocrystals (CNC) dispersions-Premises for use of CNC in enhanced oil recovery, *Ind Crop Prod*, 93 (2016) 152-160.
- [31] M.B.K. Niazi, A.A. Broekhuis, Surface photo-crosslinking of plasticized thermoplastic starch films, *Eur Polym J*, 64 (2015) 229-243.
- [32] M.B.K. Niazi, M. Zijlstra, A.A. Broekhuis, Understanding the role of plasticisers in spray-dried starch, *Carbohydr Polym*, 97 (2013) 571-580.

- [33] X.Z. He, T.J. Kim, M.B. Hägg, Hybrid fixed-site-carrier membranes for CO₂ removal from high pressure natural gas: Membrane optimization and process condition investigation, *Journal of Membrane Science*, 470 (2014) 266-274.
- [34] A. Mandal, D. Chakrabarty, Studies on the mechanical, thermal, morphological and barrier properties of nanocomposites based on poly(vinyl alcohol) and nanocellulose from sugarcane bagasse, *J Ind Eng Chem*, 20 (2014) 462-473.
- [35] J. Sriupayo, P. Supaphol, J. Blackwell, R. Rujiravanit, Preparation and characterization of alpha-chitin whisker-reinforced chitosan nanocomposite films with or without heat treatment, *Carbohydr Polym*, 62 (2005) 130-136.
- [36] S. Kobayashi, K.D. Suh, Y. Shirokura, T. Fujioka, Viscosity Behavior of Poly(Vinylamine) and Swelling-Contraction Phenomenon of Its Gel, *Polym J*, 21 (1989) 971-976.
- [37] L.Y. Deng, T.J. Kim, M.B. Hägg, Facilitated transport of CO₂ in novel PVAm/PVA blend membrane, *Journal of Membrane Science*, 340 (2009) 154-163.
- [38] X. He, M.B. Hägg, Investigation on Nanocomposite Membranes for High Pressure CO₂/CH₄ Separation, *J Membr Sci Technol*, 7 (2017).
- [39] T.J. Kim, H. Vralstad, M. Sandru, M.B. Hägg, Separation performance of PVAm composite membrane for CO₂ capture at various pH levels, *Journal of Membrane Science*, 428 (2013) 218-224.
- [40] M. Gholami, T. Mohammadi, S. Mosleh, M. Hemmati, CO₂/CH₄ separation using mixed matrix membrane-based polyurethane incorporated with ZIF-8 nanoparticles, *Chemical Papers*, 71 (2017) 1839-1853.
- [41] N. Jusoh, Y.F. Yeong, K.K. Lau, A.M. Shariff, Transport properties of mixed matrix membranes encompassing zeolitic imidazolate framework 8 (ZIF-8) nanofiller and 6FDA-

durene polymer: Optimization of process variables for the separation of CO₂ from CH₄,
Journal of Cleaner Production, 149 (2017) 80-95.

[42] M.W. Anjum, B. Bueken, D. De Vos, I.F. Vankelecom, MIL-125 (Ti) based mixed
matrix membranes for CO₂ separation from CH₄ and N₂, Journal of Membrane Science, 502
(2016) 21-28.

[43] O.G. Nik, X.Y. Chen, S. Kaliaguine, Functionalized metal organic framework-polyimide
mixed matrix membranes for CO₂/CH₄ separation, Journal of membrane science, 413 (2012)
48-61.